JOURNAL OF MATERIALS SCIENCE 36 (2001) 4443–4457

Factors affecting the adsorption of stabilisers on to carbon black (flow micro-calorimetry studies)

Part III *Surface activity study using acid/base model probes*

J. M. PEÑA, N.S. ALLEN*, C. M. LIAUW, M. EDGE
Department of Chemistry and Materials, Manchester Metropolitan University, Chester Street, Manchester MI GD, UK
E-mail: n.allen@mmu.ac.uk

B. VALANGE
Cabot Corporation, Rue Prevochamps 78, 4860 Pepinster, Belgium

F. SANTAMARÍA
Department of Chemistry and Materials, Manchester Metropolitan University, Chester Street, Manchester MI GD, UK

The first and second part of this series of papers investigated the interaction between carbon black and stabilisers (phenolic antioxidants and HALS, respectively) and showed that the mechanism was dependent on both the chemical nature of the carbon black surface and the molecular structure of stabilisers. In this third part, the interactions between model compounds, of varying acidity, and the same four carbon blacks, are investigated using flow micro-calorimetry (FMC) and Fourier transform Infrared spectroscopy (FTIR). As with the first and second parts, differences in adsorption behaviour between the four types of carbon black were evident and were principally related to the chemical nature of the surfaces and the adsorbates. In this study further insight in to the nature of the interactions between the carbon black surface functional groups and the acidic and basic probes has been acquired. The main forms of interaction are hydrogen bonding and Lewis and Bronsted acid/base interactions, formation of proton transfer complexes was also considered possible in cases of strong adsorption. The adsorption behaviour of acid and basic aromatic probes, together with octadecanol and stearic acid, was also found to be dependant on the carbon black surface topography. Flat graphene layers containing minimal heteroatoms favoured adsorption of the latter species as flat adsorption and/or structural ordering was permissable.

1. Introduction

The first and second parts of this series of papers[1, 2] describe adsorption studies of hindered phenol antioxidants and hindered amine light stabilisers (HALS) on to four different carbon blacks. These papers have advanced the understanding of how variations in stabiliser structure can affect adsorption onto carbon black. The four carbon blacks investigated differed mainly in terms of the surface concentration of oxygen containing functional groups and surface topography. Extensive surface chemical characterisation of these four carbon blacks, via XPS, FTIR and N_2 BET adsorption studies, is reported in the first part.

In the study reported here, we aim to examine the interaction between the surface functional groups of carbon black and the functional groups of model compounds such as simple 1°, 2°, and 3° aliphatic and aromatic amines and simple alcohols, esters and carboxylic acids. The data from this investigation will afford a more precise understanding of these interactions and how they are affected by the distribution and surface concentration of carbon black functional groups and simple variations in adsorbate molecular structure. The latter variation includes changes in alkyl group chain length and aliphatic/aromatic character.

The adsorption of molecules on to carbon black and graphite surfaces has attracted much attention in the literature due to implications in terms of polymer reinforcement [3, 4] and the adsorption of polymer additives [5]. Any adsorption study must include a thorough survey of the surface chemistry of the substrate. However, the very complex physical structure of carbon black and the presence of numerous oxygen containing functional groups severely complicates the surface analysis of such materials.

In general, furnace blacks contain 9 mg of oxygen per 100 m^2 of surface area [6] and as much as 1.2% combined sulphur, together with a few tenths of a percent

* Author to whom all correspondence should be addressed.

(sometimes as high as 1%) ash. The ash consists of the salts and oxides of calcium, magnesium, sodium, and in some products potassium. This ash accounts for the basic pH (8–10) commonly found in furnace blacks [6]. Whilst the hydrogen and sulphur are distributed on the surface and the interior of the aggregates, the oxygen is located on the surface as oxygen containing functional groups. The surface oxygen content has been found to be mainly in phenolic groups [6], however, other functional groups including carboxyl, phenols, lactones, aldehydes, ketones, quinones, hydroquinones, anhydrides and ethereal structures, have also been identified.

The functional groups described above (carboxylic acid, phenolic, quinone and lactones groups) are believed to be attached to the edges of the graphitic layers. These groups can interact with elastomers and plastics as well as others additives such as plasticisers and stabilisers. Small molecules can be adsorbed on the surface of the carbon black. By measuring the heat of adsorption, it has been shown that the interaction with various adsorbates is strong at very low coverage and decreases sharply at a coverage above about 0.2 of a monolayer [7]. Inverse gas chromatography (IGC) and Flow microcalorimetry (FMC) have revealed significant differences in adsorption energies and entropy depending on the shape of the hydrocarbon-adsorbate molecule and the structure and chemistry of the carbon black surface [8]. Potentiometric titration and Boehm titration has also been shown to provide useful insight into the distributions of the various acidic groups on carbon black surfaces [9].

2. Experimental

2.1. Materials

The acidic probes investigated were octadecanoic acid (stearic acid), phenol, propan-l-ol. Ethyl acetate was included in this series to examine the effect of the ester carbonyl group and ester C-O-R group on the adsorption in the absence of the active hydrogen of carboxylic acids. The basic amine probes were 2-amino butane, phenylamine, piperidine, pyridine, triethylamine and tributylamine (all probes were from Aldrich). Further details, including pK_a values and dipole moments, are given in Table I. Decahydronaphthalene was used as the non-adsorbing probe in FMC studies. The carrier fluid was HPLC grade *n*-heptane (Aldrich), stored over activated (350°C/3.5 hours) 4A molecular sieves. The liquid alcohols and esters were dried in the latter manner and the amines were dried over sodium hydroxide.

The furnace carbon blacks CB-A, CB-B, CB-C and CB-D were all supplied by the Cabot Corporation. Their principal characteristics are given in Table II. Details of their surface chemistry obtained via XPS, are described in detail in Part I, but are summarised in Tables III and IV.

The acidic and basic compounds, and carbon blacks, were chosen according their chemical nature and surface features. Only CB-A and CB-B, both used in plastic applications, were studied with all the selected probes.

2.2. Carbon black surface analysis

The carbon black XPS spectra were obtained with a SSI-X probe (SS-100/206) spectrometer from Fisons

TABLE III Surface elemental compositions of the different carbon blacks

CB sample	% C	% O	% S	% N	O/C	S/C	N/C
CB-A	99.44	0.55	0.02	0	0.0055	0.0002	0
CB-B	98.48	0.96	0.54	0	0.0097	0.0055	0
CB-C	95.54	3.73	0.34	0.39	0.0390	0.0036	0.0041
CB-D	93.8	5.77	0.23	0.18	0.0615	0.0025	0.0019

TABLE I Acid and basic probes investigated

Chemical structure	Molar mass	pK_a[a]	μ[b] (Debyes)	Chemical structure	Molar mass	pK_a[a]	μ[b] (Debyes)
Stearic acid	284.49	4.9	1.75	Secbutylamine	73.14	≥10.8	1.17
Benzoic acid		4.19		Piperidine	85.15	11.123	
Phenol	94.11	9.89	1.45	Aniline	93.13	4.63	1.53
Propan-1-ol	60.1	≥17	1.68	Pyridine	79.1	5.25	2.19
Octadecanl-ol	270.5	≥17.5	1.6	Triethyl amine	101.19	≅11	0.66
Ethyl acetate	88.11	—	1.78	Tributyl amine	185.36	≅11	0.6

[a]p$K_a$values in aqueous solution [20], for bases is the value of conjugated acid.
[b]Electric dipole moment in the gas phase [19].

TABLE II Properties of carbon blacks studied

CB type	Surface area STSA[a] (m^2g^{-1})	Surface area N_2BET (m^2g^{-1})	Particle size[b] (nm)	Iodine number (mg g^{-1})	DBPA pellets (cm^3/100 g)	Volatile, content[b] (%)	pH	Water content[c] (% wt. CB)
CB-A	86.8	107.1	22	119.6	96.6	1.5	8.5	1.01
CB-B	79.3	81.1	25	79.2	101.6	1	8.5	1.08
CB-C	85.1	113.2	25	78.2	72.5	3.5 ± 1	2.5	2.56
CB-D	370.5	542.8	13	173.3	91.3	8.5-12	2.5	8.59

[a]Standard thickness surface area.
[b]Determined by the Cabot Corporation.
[c]Obtained by Karl Fisher measurements.

TABLE IV Detailed functional composition (ratio O/C, S/C) of the different carbon blacks

Sample	O═C O─S carboxylic aldehyde, Ketone	O─C Hydroxyl, Ethers	O─C Phenol anhydride	H_2O O_2	S─C	SO_2 Sulphones	SO_4 Sulphates	C─N	NO_2
Binding energy (ev)	531.5	533.1	534.5	535.8	163.8	166.4	168.8	400	405
CB-A	0	0.0049	0	0.0006	0.0002	0	0	0	0
CB-B	0	0.0082	0	0.0006	0.0043	0.0006	0.0003	0	0
CB-C	0.0163	0.0127	0.0046	0.0024	0.0023	0.0005	0.0006	0.0027	0.0014
CB-D	0.0245	0.0238	0.0068	0.0037	0.0008	0	0.0016	0.0019	0

(Surface Science Laboratories, Mountain View, CA), equipped with an aluminium anode (10 kV, 17 mA) and a quartz monochromator. The direction of photoelectron collection made angles of 55° and 73°, from the normal to the sample and the incident X-ray beam, respectively. The electron flood gun was set at 6 eV. The vacuum in the analysis chamber was 2.5×10^{-7} Pa. The binding energies of the peaks were determined by setting the C (ls) component due to carbon only bound to carbon and hydrogen at a value of 284.2 eV. The peak areas were determined with a non-linear background subtraction. Intensity ratios were converted into atomic concentration ratios by using the SSI ESCA 8.3 D software package. The peaks were curve fitted using a non-linear least squares routine and assuming a Gaussian/Lorentzian (85/15) function.

Transmission FTIR was carried out on the unmodified carbon blacks and on air dried samples recovered from the FMC cell, after completion of the adsorption-desorption experiments. The samples were diluted to 0.09% carbon black with dried KBr (3 hours at 300°C), and a 0.2 g disc then pressed in the usual manner. The discs were placed in a transmission cell fitted to a Nicolet 510 FTIR spectrophotometer (DTGS detector) with dry-CO_2 free air purging. Spectra were made up of 500 scans with a resolution of 2 cm^{-1}.

Karl Fisher analysis was performed in order to determine the water content of the pure carbon blacks studied. A Kyoto MKC210 titrator coupled to an ADP-351 evaporator at 200°C was used for this work.

2.3. FMC procedures

The FMC used was a Microscal 3V that has been upgraded to the all PTFE fluid path "l" (inert) specification. The Instrument was linked to the Microscal thermistor Bridge-control unit whose output was fed to a Perkin-Elmer 900 series interface. The cell outlet was connected to a Waters 410 differential refractometer whose data was fed into the second channel of the 900 series interface. Other details are described in part 1 [1].

The basic FMC experimental conditions were conducted using a cell temperature of 27°C (±1°C) and a probe concentration of 0.03% w/v. The solvent flow rate was 3.30 cm^3 hr^{-1} and sample size was 67.5 mg (±0.5 mg). The differential refractometer had the cell temperature set at 40°C. Samples were left to equilibrate at a carrier fluid flow rate of 0.033 cm^3 hr^{-1} over night. The flow rate was then increased to 3.3 cm^3 h^{-1} and the system left to settle for ca. 1 hr. Data collection was started and after 5–10 minutes the inlet was switched from carrier fluid to the solution of the probe in the carrier fluid. After the RI data reached a stable limiting value (typically 80 to 110 minutes) the inlet was switched back to carrier fluid and the desorption processes recorded and the run terminated. Thermal calibration was carried out with 2–3 peaks (100 μW for 200 s) being generated. The differential refractometer is then calibrated using the 20 μl loop, 7–8 calibration peaks were obtained. Non-adsorbing probe data was obtained once for each carbon type. Please refer to part 1 or other publications [10] for details of data analysis.

3. Results and discussion

3.1. Characterisation of the carbon blacks

The characterisation of the black surface chemistry was carried out using X-ray photoelectron spectroscopy (XPS), FTIR, BET, lodine adsorption and Karl Fisher measurements. Additional data were supplied by the Cabot Corporation. The findings of these analyses are described in detail in Part 1 therefore only essential details will be given here.

The water content, volatile content and pH can be related to the hydrophilic character of the carbon black particle. For example, CB-D and CB-C have been oxidised with nitric acid and therfore have a higher surface concentration of oxygen containing functional groups than CB-B and CB-A. The FTIR and XPS analysis effectively confirms the latter. The differences between the STSA specific surface area and the N_2BET specific surface area can be related to the porosity of the carbon black. Data shown in Table II, together with literature data [11, 12], indicates that CB-D is likely to have a porous surface. Micro-pores (<2 nm), meso-pores and macro-pores are present in this sample and are likely to affect its adsorption behaviour.

3.1.1. FTIR and XPS studies on unmodified carbon black

For completeness the FTIR spectra of the unmodified carbon blacks are shown in Fig. 1. The major findings will only be summarised here as a more detailed interpretation is given in Part 1. It is immediately evident that only the oxidised samples CB-C and CB-D show obvious evidence of carbonyl species (at about 1730 cm^{-1}), with CB-D showing the slightly stronger absorption. CB-A and CB-B do not show any IR spectral evidence of carbonyl species. All samples show a broad O─H stretching band, which can be assigned to adsorbed water. It is also important to note that the

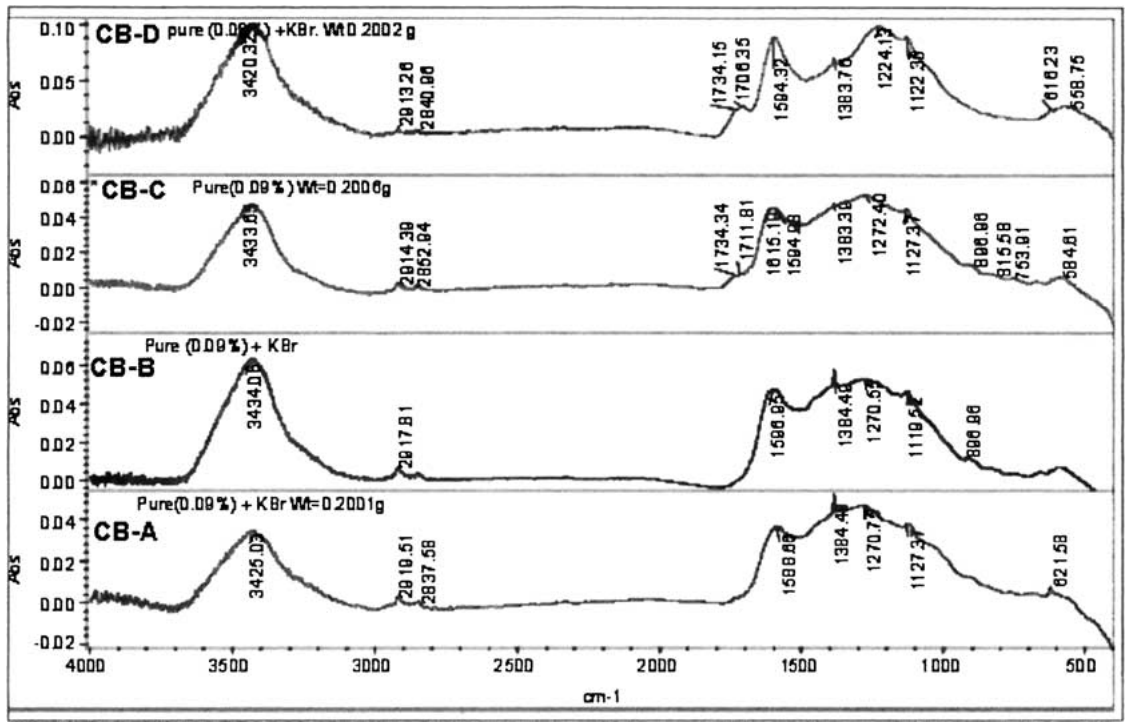

Figure 1 FTIR spectra of unmodified CB-B, CB-A, CB-C and CB-D, pure carbon blacks.

broad band centred at 1600 cm^{-1}, mainly arising from the polyaromatic structure of the carbon black, has been shown to hide some carbonyl (i.e., carboxylates and α, β-unsaturated carbonyls) and phenolic species which are potentially detectable by XPS.

The XPS data generally confirms the IR data but provides far more detailed information on the surface chemistry. The results are summarised in Tables III and IV. The oxygen content can be ranked as follows and is in the ratio 1.00:1.75:6.78:10.49, for CB-A, CB-B, CB-C and CB-D, respectively. Only CB-C and CB-D show evidence of carbonyl species (in the ratio of 1.00:1.50), such as carboxylic acids, aldehydes and ketones. Such species reflect the strongly oxidising treatments to which these samples have been subjected. CB-A to CB-D show evidence of hydroxyl and ether oxygen in the ratio ranking of 1.00:1.67:2.59:4.86, respectively. CB-B has the highest level of sulphur, mainly in the form of S–C species, reflecting the relative impurity of the oil feed stock used to produce this sample.

3.2. Adsorption studies

The results are presented as a histogram showing adsorption and desorption data for each probe. In order to facilitate comparison of the data, the sign of the exothermic adsorption energy change is reversed.

3.2.1. Adsorption energies of amine probes

Adsorption and desorption energies resulting from the interactions of the different basic probes with the carbon blacks were estimated by the FMC procedure (Figs 2 and 3). The basicity of these probes can be ranked as follows:

$$\text{piperidine} \geq (\text{triethylamine} = \text{tributylamine}) > \text{2-aminobutane} > \text{pyridine} > \text{aniline}.$$

Piperidine (2° amine) shows a higher adsorption/desorption energy than 2-amino butane, thus implying that piperidine can be adsorbed via hydrogen bonding or acid-base reactions more easily than 2-aminobutane. The greater basicity of piperidine [13], relative to 1° amines, together with its more compact and simpler structure, allows intimate contact with the carbon black surface with the result that the strength (and hence energy) of the interaction is maximised. In general the greater the basic character of a model compound the greater will be the adsorption activity on a given carbon black.

The inductive effect of the benzene ring of aniline, reduces its basic character, relative to 2-aminobutane, and hence its adsorption energy. As the 3° amines, triethylamine and tributylamine, are aliphatic they are more basic than 2-aminobutane but almost equal in basicity to piperidine. Hence, the adsorption energies of triethylamine and tributylamine are higher than that of pyridine on to CB-D, and CB-B. On CB-C, only triethylamine, has a higher adsorption energy than pyridine. For CB-C, and CB-A, the adsorption energy of tributylamine is lower than that of pyridine.

Therefore as expected, piperidine being the most basic probe shows the higher adsorption activity with CB-D, CB-B, and CB-A. For these carbon blacks the adsorption activity of the probes used can be ranked according to their decreasing basic character, as follows:

$$\text{piperidine} > \text{2-aminobutane} > \text{Pyridine}.$$

Despite the higher basicity of pyridine, relative to aniline, the adsorption energy of pyridine on to CB-B and CB-A, was lower than that of aniline. This discrepancy indicates that interactions in addition to acid-base type, contribute to the adsorption energy of aniline onto these substrates. It is likely these extra energy contributions could be associated with hydrogen bonding and

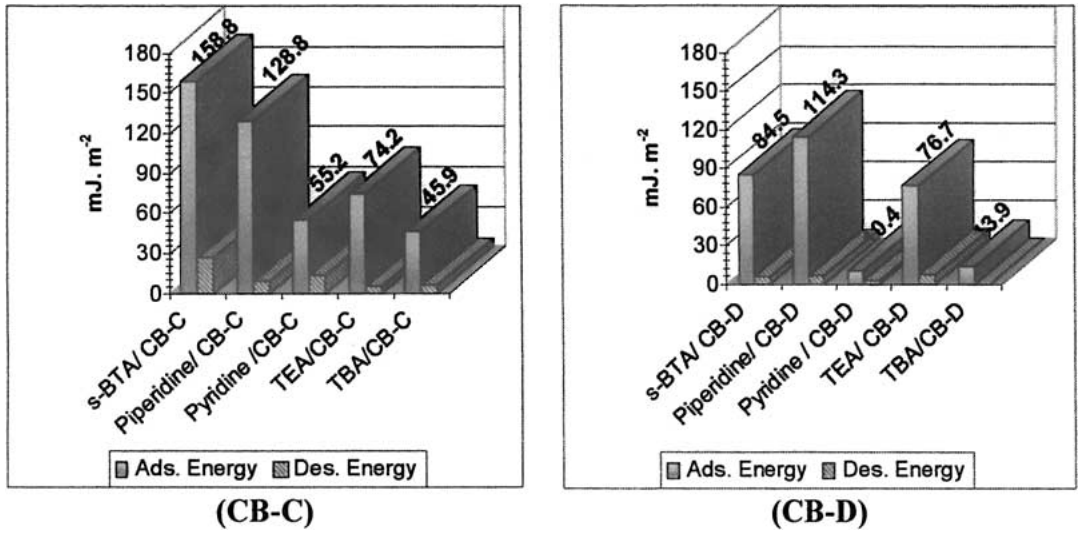

Figure 2 Adsorption energies for amine model compounds on CB-C and CB-D.

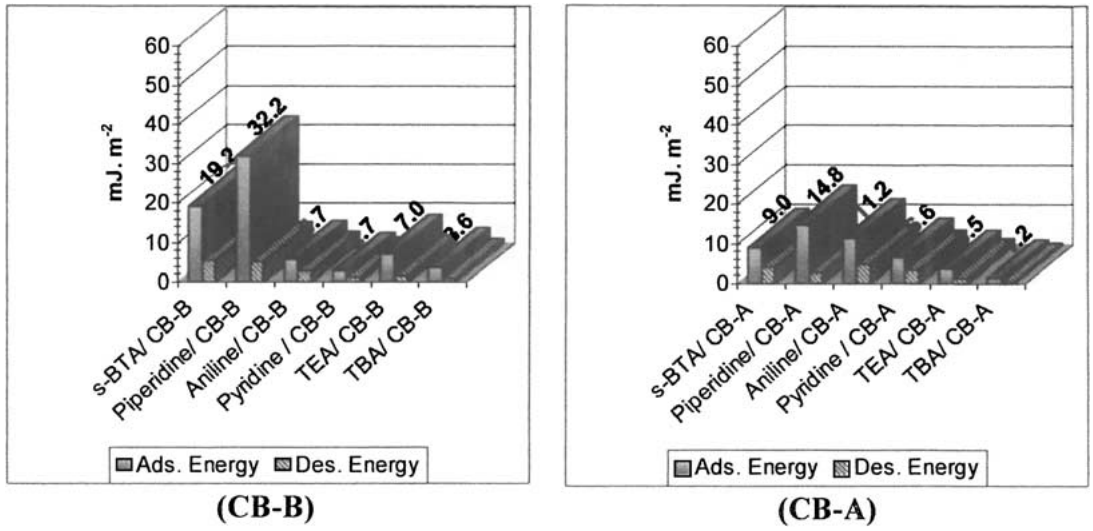

Figure 3 Adsorption energies for amine model compounds on CB-B and CB-A.

dispersive interactions involving the aromatic ring of the aniline and the polyaromatic structures on the carbon black surface.

Differences between triethylamine and tributylamine show that occupied molecular are is also a factor affecting the adsorption activity of the basic model compounds (Figs 2 and 3). Calculation of heat of adsorption per molecule for these probes yields similar values, thus showing that the nature of interaction is the same.

CB-C Gives a different ranking of adsorption energy:

2-aminobutane > piperidine > pyridine.

The adsorption energy trends of all four carbon blacks are identical with piperidine, 2-aminobutane and pyridine, the following ranking exists:

CB-C > CB-D > CB-B > CB-A.

For instance with piperidine the values obtained are:

(128.8 mJ m^{-2}) > (114.3 mJ m^{-2}) > (32.2 mJ m^{-2}) > (14.8 mJ m^{-2})

This ranking can be partially explained by the acidity of the carbon blacks, which can be ranked as follows:

CB-D ≥ CB-C > CB-B > CB-A (Tables II and IV).

The difference in adsorption activity between the four carbon blacks towards the basic compounds further highlights the differences in structure and surface chemistry. The adsorption activity of a carbon black towards basic and nucleophilic amine probes is likely to be governed by the surface concentration of acidic functional groups. The surface concentration of acidic oxygen containing functional groups, arising from strongly oxidising treatments of carbon black, can be correlated with the volatile content of carbon black concerned [6]. Thus, according to the XPS analysis reported in Tables III and IV, CB-C has a greater surface concentration of acidic functional groups than CB-B and CB-A.

However, CB-D has by far, the highest volatile content (8.5–12%, Table II) and surface oxygen content (5.8%, Table III), and is very acidic when dispersed in water (pH of 2.5 ± 1), though unexpectedly, the

adsorption energies of 2-aminobutane piperidine and tributylamine, on CB-D are lower than on CB-C. The XPS data clearly shows that CB-D has the most highly functionalised surface of all the samples examined. As with the previous two investigations on hindered phenolic antioxidants [1] and HALS [2] this data is at odds with the area normalised adsorption energy data obtained from the FMC, which shows that CB-C has the most active surface. This effect is likely to be due to two factors; the first is associated with strongly adsorbed water molecules on and around the surface functional groups, i.e., the so called "hydrogel effect". These adsorbed water molecules become involved in a hydrogen bonded network which effectively blocks access to the adsorption site [14, 15], thus resulting in a reduction of adsorption energy. The second factor is mutual interaction between adjacent functional groups such that the mutual interactions are preferred to interactions with the adsorbate molecules. It can therefore be envisaged that a critical average distance between functional groups (hence critical surface concentration) must be reached before mutual interaction and the hydrogel effect becomes a significant factor. In the case of CB-D this critical surface concentration has been reached or exceeded.

There are also differences, however, in the nature of the functional groups present on each carbon black surface and their population distribution. CB-C has oxidised functional groups like SO_4 and C═O (carbonyls and carboxyls) whilst CB-B has mainly O─C and S─C (i.e., alcohols and thiols). The concentrations of sulphates and sulphones are very low (10 times lower than the former ones). Their contributions are probably negligible. Therefore, the difference between CB-A and CB-B can be justified by the difference in O─C and S─C concentration. This is consistent with the type and relative impurity of the oil feedstock used to produce CB-B, which has a higher sulphur and oxidised hydrocarbon content than that used to produce CB-A. Hence, taking into account the XPS analysis and the BET surface analysis, CB-B has a greater concentration of functional groups than CB-A and therefore a higher overall adsorption activity.

However, the above reasoning does account properly for the difference in adsorption energy values of aniline and pyridine on to CB-B and CB-A; CB-A is more active with aniline and pyridine than CB-B. This suggests that the adsorption mechanism of these probes can involve an alternative form of interaction, perhaps together with the acid/base interaction and hydrogen bonding. CB-A is the purest sample examined and is therefore likely to have flat and uncluttered graphene basal planes, which are likely to provide a more suitable environment for flat adsorption of the planar aniline and pyridine molecules, via dispersive interactions. These dispersive interactions are likely to contribute significantly to the adsorption energy, thus causing CB-A to show greater activity with these probes than CB-B, where only acid base interaction and hydrogen bonding may be possible.

With triethylamine and tributylamine, the order of surface activity of CB-A and CB-B is as expected, on the basis of the surface acidity ranking. The nitrogen atom in these probes is sterically hindered by the alkyl groups, and therefore results in a reduction in the ability to form hydrogen bonds. This means that acid-base interactions are likely to form the major contribution to the adsorption energy. Due to their shape, these 3° amines will not be able to interact strongly with the flat graphene basal planes of CB-A.

In summary, acid/base interactions, together with hydrogen bonding and dispersive interactions must be considered when the interactions between basic additives and carbon black are studied. The relative contributions of each of these interactions is dependent on the shape the adsorbate molecule and the chemical nature and surface topography of the substrate.

With an acidic carbon black, that has surface groups such as carboxylic acids, phenols and sulphur containing groups, interactions with adsorbates can be via both acid-base interactions and hydrogen bonding; whilst with surface groupings such as esters, quinones and lactones, hydrogen bonding predominates. This can be seen in the FTIR results (shown later), where an absorption frequency shift to lower energy is observed for the carbonyl absorptions (Figs 10 to 13).

In general, the desorption energy values found were lower than the respective adsorption energy values. The difference between these values relates to the degree of retention of the probe on the surface, and hence the reversibility of the adsorption mechanism. CB-C and CB-D showed stronger retention of the probes than the other carbon blacks, due to their high acidity and surface porosity. In cases in where the relative acid-base strength of the absorbent and adsorbate is increased, increasing adsorption irreversibility can be predicted, because a stronger bond will form between the two species [16].

3.2.2. Adsorption energies of carboxylic acids alochols and ethyl acetate

Adsorption and desorption energies resulting from the interactions of the different acidic probes with the carbon blacks were determined by the FMC procedure. Figs 4 and 5 show that, in general the greater acidic character of a model compound results in greater adsorption activity on a given carbon black, with the exception of stearic acid, which shows lower adsorption activity than phenol.

The acidic character of the additives used can be ranked as follows:

benzoic acid ($pK_a \approx 4.2$) > stearic acid ($pK_a \approx 5$) > phenol ($pK_a \approx 10$) > propan-1-ol ($pK_a \approx 17$–16) ≥ octadecanol ($pK_a \approx 17$–16).

Ethyl acetate obviously has no pK_a value, but will be able to interact by dipolar interaction. Despite the fact that stearic acid has higher acidity, phenol shows the highest adsorption energy, followed by benzoic acid. This higher activity is probably due to the flat and planar aromatic structures of the latter two probes, as opposed to the C_{17} alkyl chain of stearic acid. The latter portion of the stearic acid molecule accounts for the major proportion of its molecular volume, and will have strong

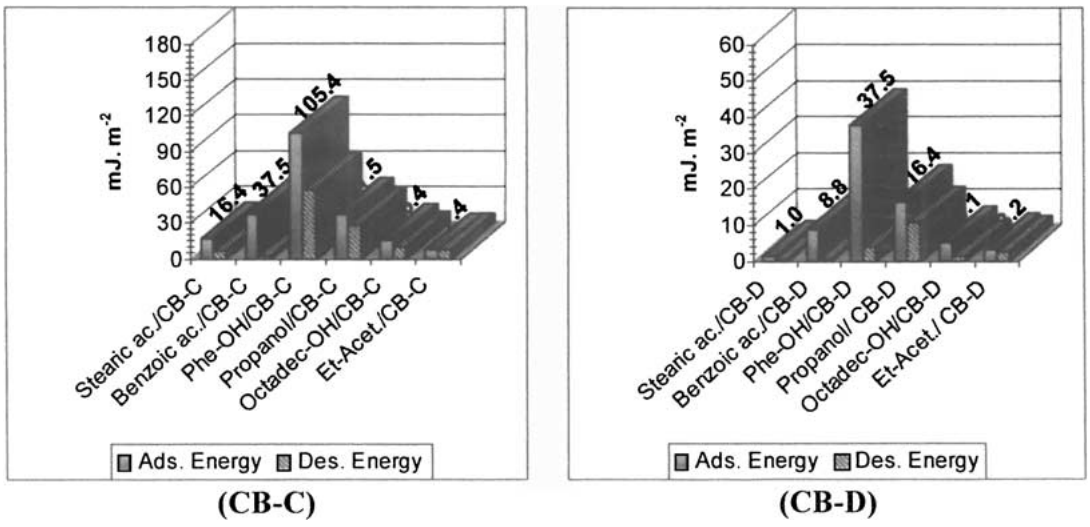

Figure 4 Adsorption energies for carboxylic and hydroxyl model compounds on CB-C and CB-D.

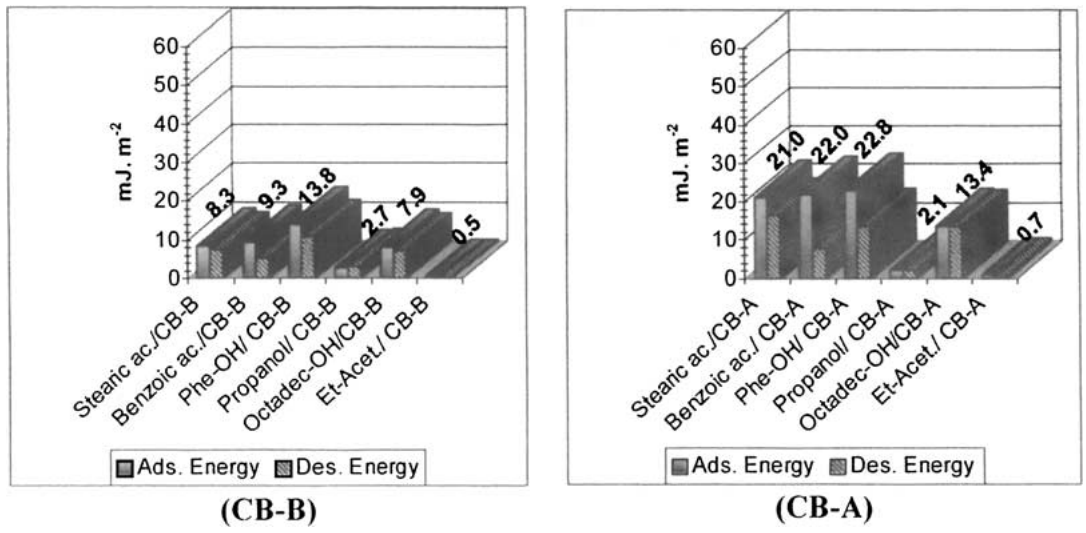

Figure 5 Adsorption energies for carboxylic and hydroxyl model compounds on CB-B and CB-A.

affinity for the heptane carrier fluid, therefore strong solvation of the alkyl chain is likely. Detachment of the solvating molecules (endothermic) during adsorption will decrease the heat of adsorption. The more compact benzoic acid and phenol molecules may also easily fit into the pores of CB-C and CB-D, thus allowing a greater surface area for adsorption. This explanation can be also applied to propanol and octadecanol; because with CB-C and CB-D, the heat of adsorption of the latter probe was noticeably less than the former one. This reasoning breaks down with CB-A and to a lesser extent with CB-B, due to the previously described surface topological differences.

Differences in the heats of adsorption of octadecanol and stearic acid afford some insight into the nature of interaction and hence the type of surface functional group with which it interacts. On CB-C, the adsorption energies of these two probes is very similar, whilst with CB-D, octadecanol is the more strongly adsorbing probe. This could be explained because of the amphoteric character of the alcohols, which may result in the octadecanol and propanol acting as bases for the relatively strong acids located on the carbon black surface [13]. Such an effect will cause the heat of adsorption to exceed that of stearic acid, which can only interact with the surface acid groups by hydrogen bonding. This explanation can also be applied to the differences observed between phenol and benzoic acid when adsorbed onto CB-D and CB-C.

With CB-A and CB-B the adsorption energies of stearic acid, phenol and benzoic acid are quite similar, this may be due to similarity in the adsorption mechanism for each of these probes. With CB-B these adsorptions were shown to be reversible which implies that hydrogen bonding and dispersive interactions are mainly involved, rather than acid-base interactions. However, with CB-A phenol and benzoic acid showed greater retention that may reflect stronger dispersive interactions, resulting from the previously described flat adsorption of these probes. In contrast, the same probes showed far stronger retention on CB-C and CB-D, therefore indicating a strong contribution from acid-base interactions.

Resonance stabilisation of the phenoxide ion causes phenol to be more acidic than aliphatic alochols, this feature enhances the adsorption activity of phenol relative to octadecanol and propanol [13]. The similar adsorption energy trends observed with phenol and

propanol, and the relative differences between propanol and stearic acid, across the four carbon blacks examined, can be explained by the differing adsorption mechanisms of these probes. Although phenol is likely to have a stronger acid-base component to its energy of interaction, relative to propanol, both these alcohols are able interact with the carbon black via hydrogen bonding. Being flat and planar with delocalised π-electrons, the aromatic ring of phenol can particpate in dispersive interactions when it is adsorbed flat on to the graphene layers of carbon black. Such effects have been discussed in the literature [17] and will further increase the energy of adsorption.

Ethyl acetate interacts weakly with carbon black via the ester grouping, which may participate in hydrogen bonding with labile hydrogen atoms of acidic sites on the carbon black surface. Such sites include carboxyl groups (evident on CB-C and CB-D, Fig. 1) and phenolic groups (Table IV). Ethyl acetate shows the weakest adsorption activity with CB-A and CB-B, due to the very low surface concentration of acidic functional groups on these samples.

With all four carbon blacks, identical adsorption energy trends are observed with phenol, propanol and ethyl acetate. The ranking is as follows:

CB-C > CB-D > CB-A > CB-B (With the exception of CB-B which shows slightly higher adsorption energy with propanol than CB-A)

The actual values of adsorption energy can be ranked as follows:

with phenol: 105.4 (mJ m^{-2}) > (37.5 mJ m^{-2}) > (22.8 mJ m^{-2}) > (13.8 mJ m^{-2}),
with propanol: (37.5 mJ m^{-2}) > (16.4 mJ m^{-2}) > (2.1 mJ m^{-2}) > (2.7 mJ m^{-2}),
with ethyl acetate: (7.4 mJ m^{-2}) > (3.2 mJ m^{-2}) > (0.7 mJ m^{-2}) $\geq$ (0.5 mJ m^{-2}).

Variation of the surface acidity (Bronsted) of the carbon blacks, cannot in it self, explain the ranking observed, as the Bronsted acidity can be ranked as follows: CB-D $\geq$ CB-C > CB-B $\geq$ CB-A. It is important to appreciate that basic groups can also be present on the surface. The carbon black surface should hence be considered amphoteric in nature. Different ratios of concentration of basic/acidic groups on the carbon black surface could explain the data presented in Figs 4 and 5. Due to the acidic character of the compounds, the higher activity of a given carbon black could be interpreted by a greater presence of selective basic active adsorption sites per unit surface area on that carbon black.

As the adsorption energy of stearic acid on to the four carbon blacks can be ranked as follows,

CB-A > CB-C > CB-B > CB-D, (21.0 mJ m^{-2}) > (16.4 mJ m^{-2}) > (8.3 mJ m^{-2}) > (1.0 mJ m^{-2}).

It may be suggested that CB-A has a higher surface concentration of basic sites than CB-C etc.

With the amine series, and as evidenced by the surface chemical analysis, CB-C is shown to have the most effectively acidic surface. However, CB-C also appears to have a significant concentration of basic sites on its surface as it shows the second highest adsorption energy with stearic acid.

The activity of CB-D appears to be once again weakened by the hydrogel effect and mutual interactions between functional groups. Whilst the high porosity of CB-D does not significantly affect the general adsorption energy trends with the acidic probes, the retention of phenol on CB-D is stronger than with any of the other samples. Such an anomaly may be due to phenol becoming trapped within the pore structure [17]. This effect is likely to be even more pronounced if the phenol is partially dissociated in some of the strongly adsorbed water on the surface of CB-D. This will in turn result in interaction between the phenoxide ion and hydrogen atoms, which form the edges of the graphene layers that make up the walls of the pores.

CB-A and CB-C show very similar behaviour with stearic acid, both interms of the adsorption energy and the level of adsorption (Figs 4 and 5). It may therefore be argued that these samples have a significant surface concentration of basic sites. The exact form of these basic sites is hard to predict, however, for CB-A at least they may be associated with the π-electron systems of the polyaromatic graphene layers, which will act a Lewis bases [6, 18]. By virtue of the relatively high purity of CB-A, the graphene layers are likely to be more perfect (i.e., flatter) than with the other samples. This may result in structural (perhaps crystalline) ordering of the adsorbate molecules, the resulting intermolecular interactions will simultaneously increase both the energy of and level of adsorption. It is also interesting to note that on CB-A, the heat of adsorption of octadecanol is substantially higher than propanol. This observation may be explained by heat of crystallisation of the alkyl tails (or increased dispersive interaction caused by horizontal adsorption) and may thus be further evidence in support of adsorption on the graphene layers. With CB-C hydrogen bonding interaction with stearic acid cannot be ruled out, though there may be some contribution from π-electron Lewis bases. Adventitious metal oxides originating from the feed stocks themselves and process water used in production of the carbon blacks could also form Bronsted basic sites.

3.2.3. Levels of adsorption of amine probes

The levels of adsorption and desorption of the amine probes (expressed as moles per unit surface area) are presented in Figs 6 and 7. In general, the observed quantities can be related to the values of adsorption/desorption energy described previously.

Onto CB-C and CB-D, 2-aminobutane is adsorbed to a higher level than piperidine despite the stronger basic character of the later (Fig. 6). The adsorption capacity of the carbon blacks with 2-aminobutane, piperidine and pyridine is ranked as follows:

2-Aminobutane: CB-C > CB-D > CB-B > CB-A (84.0×10^{-7} mol m^{-2}) > (11.6×10^{-7} mol m^{-2}) > (4.6×10^{-7} mol m^{-2}) > (0.7×10^{-7} mol m^{-2})
Piperidine: CB-C > CB-B $\geq$ CB-D > CB-A (11.3×10^{-7} mol m^{-2}) > (9.2×10^{-7} mol m^{-2}) $\geq$ (7.8×10^{-7} mol m^{-2}) > (5.0×10^{-7} mol m^{-2})

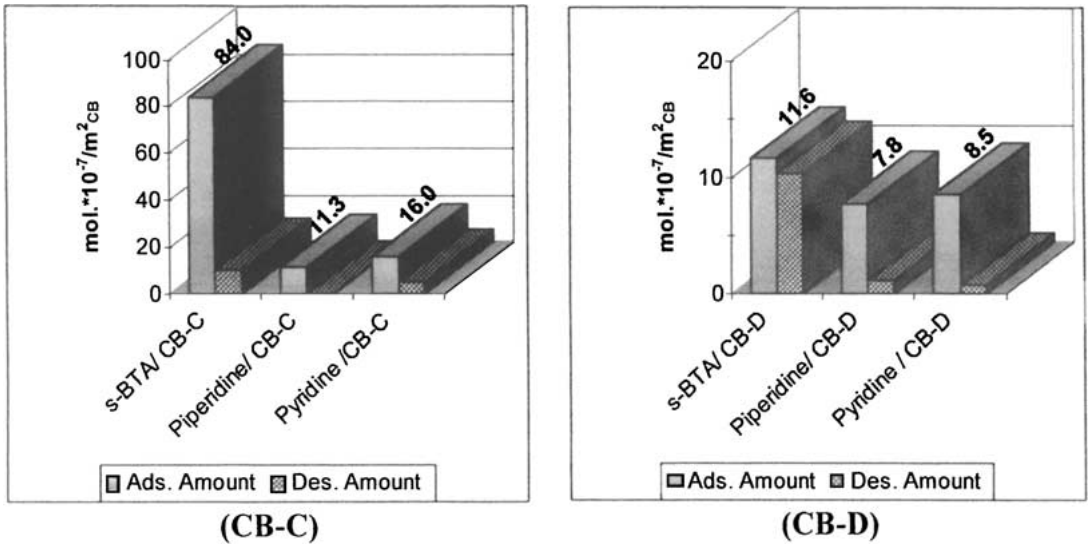

Figure 6 Levels of adsorption and desorption for amine model compounds on CB-C and CB-D.

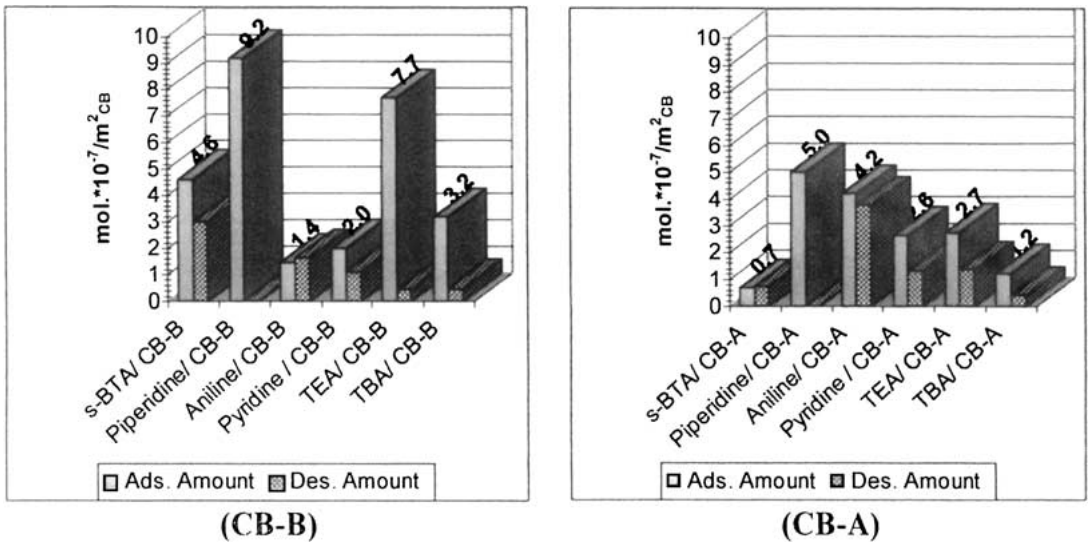

Figure 7 Levels of adsorption and desorption for amine model compounds on CB-B and CB-A.

Pyridine: CB-C > CB-D > CB-A ≥ CB-B (16.0×10^{-7} mol m^{-2}) > (8.5×10^{-7} mol m^{-2}) > (2.6×10^{-7} mol m^{-2}) ≥ (2.0×10^{-7} mol m^{-2})

It can be concluded that with the amine series, CB-C has the most adsorption active surface, despite the fact that the XPS and FTIR data indicates the highest surface concentration of acidic functional groups on CB-D. This observation can again be explained by the hydrogel effect and mutual interaction between functional groups, which serves to reduce the interaction with adsorbate molecules, thus resulting in both reduced energy and level of adsorption.

The higher level of adsorption of pyridine on to CB-C and CB-D, than piperidine, can be explained by differing adsorption mechanisms. As piperidine is more basic than pyridine, it can interact with surface functional groups via both hydrogen bonding and acid/base interactions, resulting in higher adsorption energy than pyridine. However, pyridine has a greater dipole moment (2.26 D) than piperidine (1.57 D), and by virtue of the delocalised π-electron system of the aromatic ring, less, specific dispersive interactions can occur with the carbon black surface. Therefore resulting in a greater number of pyridine molecules being adsorbed but with less energy per molecule being liberated.

The levels of adsorption and desorption are directly related to the adsorption energies (Fig. 7) as CB-B and CB-A showed somewhat lower levels of adsorption than CB-C and CB-D.

Surprisingly aniline and pyridine show higher adsorption levels with CB-A, an effect which may be related to flat adsorption of these probes via dispersive interactions with the more perfect graphene layers of CB-A, relative to CB-B with its higher oxygen and sulphur content.

The higher surface concentration of C–O species, associated with ethers and phenols, together with the highest concentration of S–C containing species on CB-B (obtained from XPS data [1] and Tables III and IV), is reflected in its increased adsorption activity with basic probes, relative to CB-A. This shows that the

phenolic species in particular may act as acidic sites, possibly with some hydrogen bonding contribution. As the concentration of S-C species is substantially higher than for the other samples, the contribution of dispersive interactions with such species may be significant.

The increased molecular area of tributylamine relative to triethylamine, resulted in the former showing a lower adsorption energy which was in turn, governed by the lower level of adsorption. As the heats of adsorption per molecule are similar for both 3° amines, the nature of interaction is the same for both and is thus predictably unaffected by the doubling in length of the alkyl groups.

The low levels of desorption, and low desorption energies, relative to the levels of adsorption and adsorption energy, reflect significant retention of the basic probes on the carbon black surfaces. It is likely that acid-base interactions predominate, particularly in cases where the level of water retained on the carbon black surface in the FMC may be significant (i.e., CB-C and CB-D). It must be appreciated, however, that the non-polar nature of heptane will result in poor solvation of the polar components of the probes. Therefore these species may interact via interactions that range in strength from hydrogen bonding (A–H- - -B) to ion pair formation (A^{-}- - -H–$^{+}$B), via a proton transfer mechanism. Such a proton transfer mechanism may be expected between poorly solvated probe molecules and phenolic based surface functional groups, provided that the acidity of the proton donor and/or the basicity of the proton acceptor are sufficiently strong [16]. According to Vinogradov's book on hydrogen bonding [16], formation of hydrogen bonding and the latterly described proton transfer complexes, can be observed by FTIR and UV spectroscopy. Solutions of bases mixed with acidic compounds; for example, propylamine and 4-methylphenol, in CCl_4, effectively illustrate such effects. Hydrogen bonding is usually in equilibrium with ion pair complex formation, the position of this equilibrium is dependent on the polarity of the solvent and resultant degree of solvation of the active functional group in the transfer complex [16].

3.2.4. Level of adsorption of carboxylic acids alcohols and ethyl acetate

Levels of adsorption and desorption of the different acidic probes on the carbon blacks were estimated by the FMC procedure (Figs 8 and 9). As with basic probes, the levels of adsorption are generally related to the values of the adsorption energy previously described (Figs 4 and 5).

For adsorption of phenol and propanol, CB-C and CB-D show the same trend in level of adsorption, which is as follows:

CB-C > CB-D > CB-A > CB-B, Phenol: $(30.8 \times 10^{-7}$ mol $m^{-2}) > (11.4 \times 10^{-7}$ mol $m^{-2}) \geq (5.2 \times 10^{-7}$ mol $m^{-2}) > (2.0 \times 10^{-7}$ mol $m^{-2})$, Propanol: $(14.1 \times 10^{-7}$ mol $m^{-2}) > (13.3 \times 10^{-7}$ mol $m^{-2}) \geq (3.1 \times 10^{-7}$ mol $m^{-2}) > (2.6 \times 10^{-7}$ mol $m^{-2})$.

This similarity in response is likely to be due to the fact that these samples have both been oxidised by nitric acid treatment. With CB-D in particular, fairly strong retention of these probes is observed and is a reflection of its Bronsted acidity. CB-C retains these probes somewhat less strongly due to the proportion of weaker interactions with these probes. CB-A and CB-B adsorb these two alcohols more weakly and thus the adsorption is generally reversible in nature, however, CB-A shows some retention of phenol. The latter effect may be due to the flat adsorption of phenol, via dispersive interactions, as discussed earlier.

More than twice as much phenol adsorbed onto CB-A than CB-B whereas the level of adsorption of propanol onto CB-A was only very slightly greater than with CB-B. Comparison of the heats of adsorption per molecule for phenol shows that CB-B has the highest energy adsorption sites for this probe. However, these sites are present at such a low concentration that the level of phenol adsorption cannot compete with the oxidised samples which adsorb this probe to higher levels but with lower energy per molecule. CB-A also

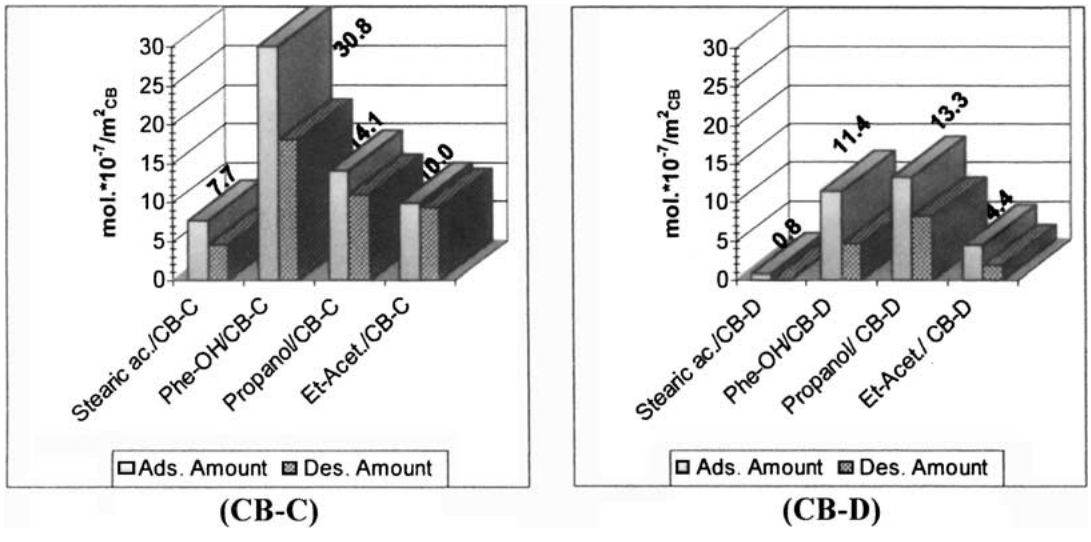

Figure 8 Levels of adsorption and desorption for carboxylic and hydroxyl model compounds on CB-C and CB-D.

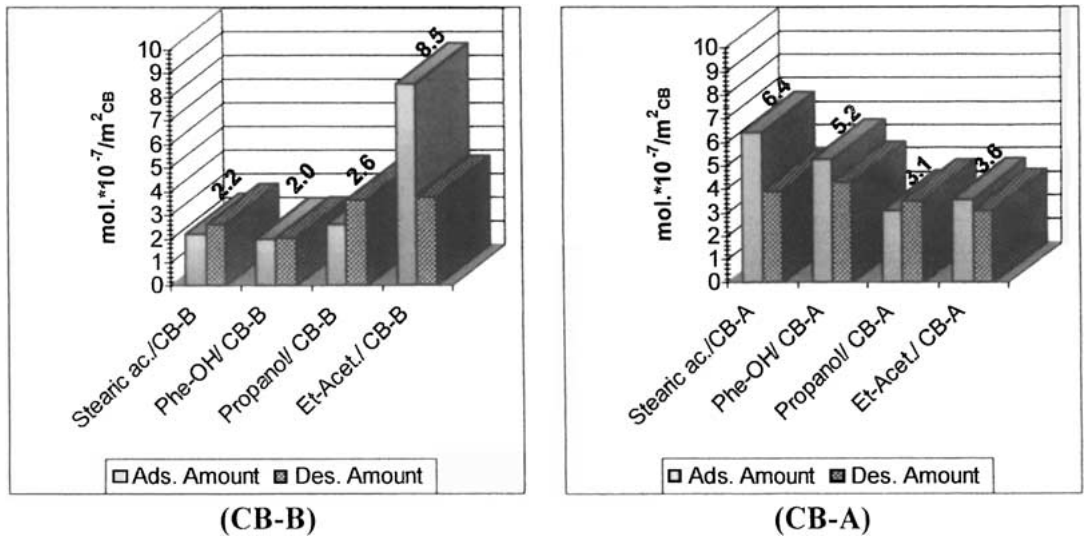

Figure 9 Levels of adsorption and desorption for carboxylic and hydroxyl model compounds on CB-B and CB-A.

adsorbs phenol molecules with energy ca. 11 kJ mol^{-1} higher than CB-C. These anomalies may be explained by unique features of CB-A and CB-B that may affect the mechanism of adsorption. CB-B has a very high level of C-S species on its surface (Table IV). The sulphur atoms may be able to interact dispersively with the aromatic ring of phenol resulting in additional contributions to the adsorption energy. CB-A is the purest sample and may have the most perfect graphene layers that may enable close, flat adsorption of the phenol molecules, thus maximising energy from dispersive interactions.

In the case of propanol, however, the gradation in heat of adsorption per molecule mirrors that for adsorption energy, this observation would be expected on the basis of the XPS data for oxygen containing functional groups (Table IV), and the hydrogel effect associated with CB-D. This behaviour indicates interaction of phenol via hydrogen bonding and acid-base interaction. The reversible adsorption character of the aliphatic alcohols can be related to their amphoteric character, with increasing reversibility with decreasing acidity of carbon blacks. Features such as sulphur content and surface topology do not significantly affect the adsorption of propanol.

The level of adsorption of stearic acid can be ranked as follows:

CB-C $\geq$ CB-A $>$ CB-B $>$ CB-D (7.7×10^{-7} mol m^{-2}) $\geq$ (6.4×10^{-7} mol m^{-2}) $>$ (2.2×10^{-7} mol m^{-2}) $\geq$ (0.8×10^{-7} mol m^{-2})

This is related to the adsorption energy trends with stearic acid which are as follows:

CB-A (21.0 mJ m^{-2}) $\geq$ CB-C (16.4 mJ m^{-2}) $>$ CB-B (8.3 mJ m^{-2}) $>$ CB-D (1.0 mJ m^{-2})

Although, CB-A showed greater adsorption energy (both per unit area and per molecule), CB-C afforded, by a small margin, the highest level of stearic acid adsorption. Interestingly CB-B showed the highest adsorption energy per molecule, this may be due to contributions from sulphur containing functional groups and possibly basic metal oxides which may be present at low concentration. The similarly high adsorption energy per stearic acid molecule observed for CB-A may be related to structural ordering of groups of stearic acid molecules adsorbing on the flat graphene layers on CB-A. However, the contribution of metal oxides that may contribute to the slightly basic pH of CB-A and CB-B (Table II) may be the dominant factor influencing adsorption of stearic acid.

Levels of adsorption of ethyl acetate can be ranked as follows:

CB-C $>$ CB-B $>$ CB-D $>$ CB-A, (10.0×10^{-7} mol m^{-2}) $>$ (8.5×10^{-7} mol m^{-2}) $>$ (4.4×10^{-7} mol m^{-2}) $\geq$ (3.6×10^{-7} mol m^{-2}).

With the exception of CB-B the adsorption of ethyl acetate was mainly reversible. This recurring anomalous behaviour of CB-B may be due to dispersive interactions associated with the high level of sulphur containing functional groups. Dipole-dipole and hydrogen bonding interactions with the oxygen containing functional groups of CB-C explain the high level of adsorption onto CB-C. The excessive surface concentration of functional groups on CB-D gives rise to the previously described hydrogel effect and mutual interactions between functional groups which act to reduce interaction with adsorbate molecules and hence the level of adsorption.

3.3. FTIR spectra on FMC modified carbon black

Samples recovered from the FMC after adsorption-desorption processes, where analysed as previously described by FTIR. The later spectra are displayed together with spectra of both the unmodified carbon black and the pure adsorbate in order to aid identification of IR absorptions associated with the adsorbate molecules. Generally the IR absorptions on even the most strongly samples appear weak, but in some cases absorptions from probe molecules could be identified on the more weakly adsorbing carbon blacks. To avoid presentation of an excessive number of spectra, data for CB-D which

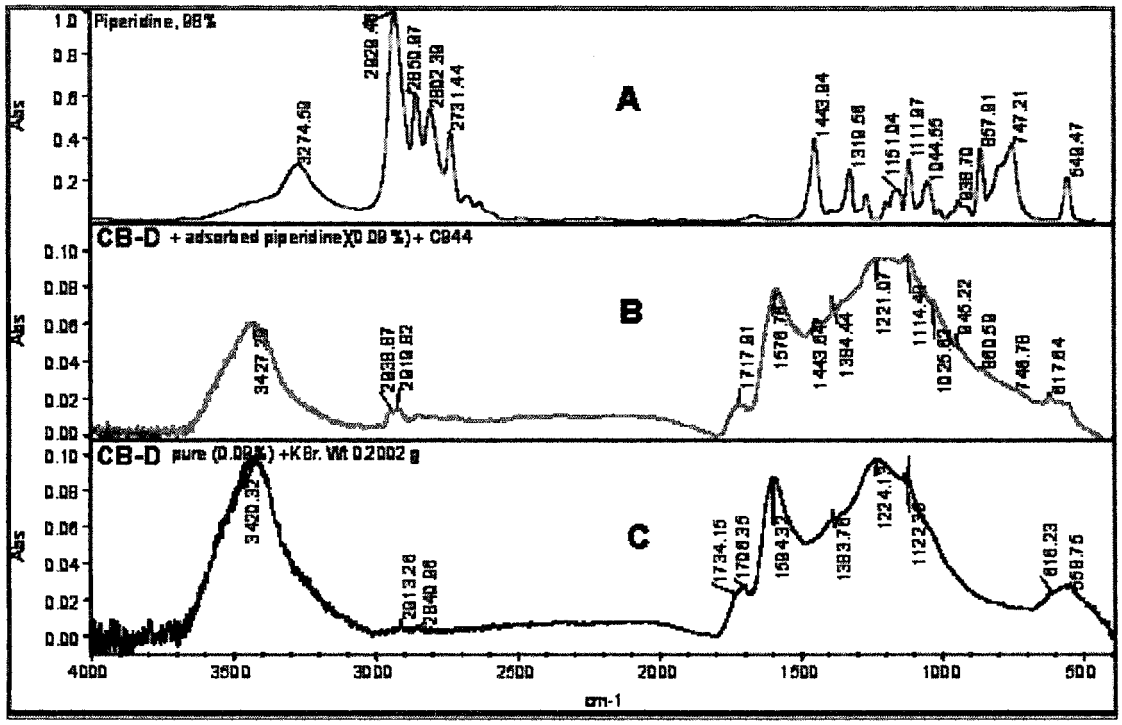

Figure 10 FTIR spectra of (a) piperidine, (b) CB-D treated in the FMC with piperidine and (c) pure CB-D.

generally showed the highest levels of adsorption per unit mass, will only be shown.

3.3.1. FTIR spectra of carbon black treated in the FMC with amine model compounds

Very weak piperidine absorptions are evident on CB-D and to a lesser extent on CB-C (Fig. 10). The main absorption were at 2930 cm^{-1} (C–H stretching vibrations of of CH_2), 1569 cm^{-1}, 1443 cm^{-1}, 1114 cm^{-1} and 750 cm^{-1} (N–H wagging in secondary amines). Due to the low levels of piperidine adsorbed on CB-A and CB-B, no absorptions from this probe could be resolved.

As with piperidine, there are some weak 2-aminobutane absorptions on FMC treated CB-D and CB-C (Fig. 11) at 2950 cm^{-1}, 1459 cm^{-1}, ca. 1380 cm^{-1} and 1160 cm^{-1}. No absorptions from 2-aminobutane could be resolved on CB-A and CB-B due to the levels of adsorption being too low.

Some insight into the mode of adsorption of 2-aminobutane and piperidine can be acquired from the IR spectral data; a barely discernible but nevertheless potentially important, broadening to lower energy is observed in the carbonyl absorption associated with the

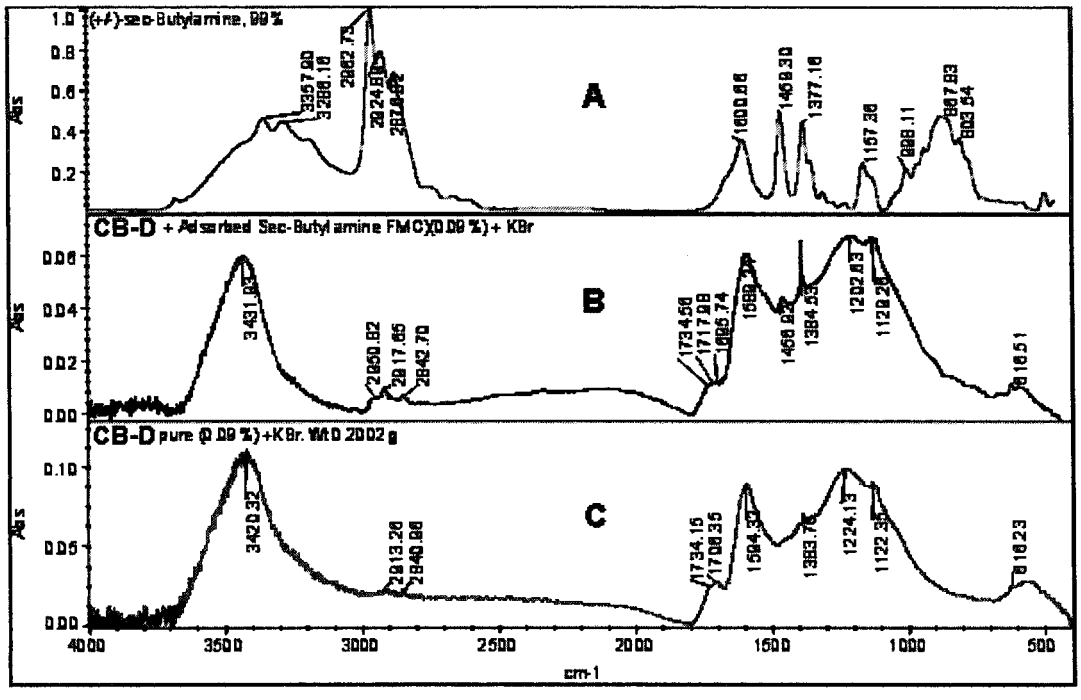

Figure 11 FTIR spectra of (a) 2-aminobutane, (b) CB-D treated in the FMC with 2-aminobutane and (c) CB-D.

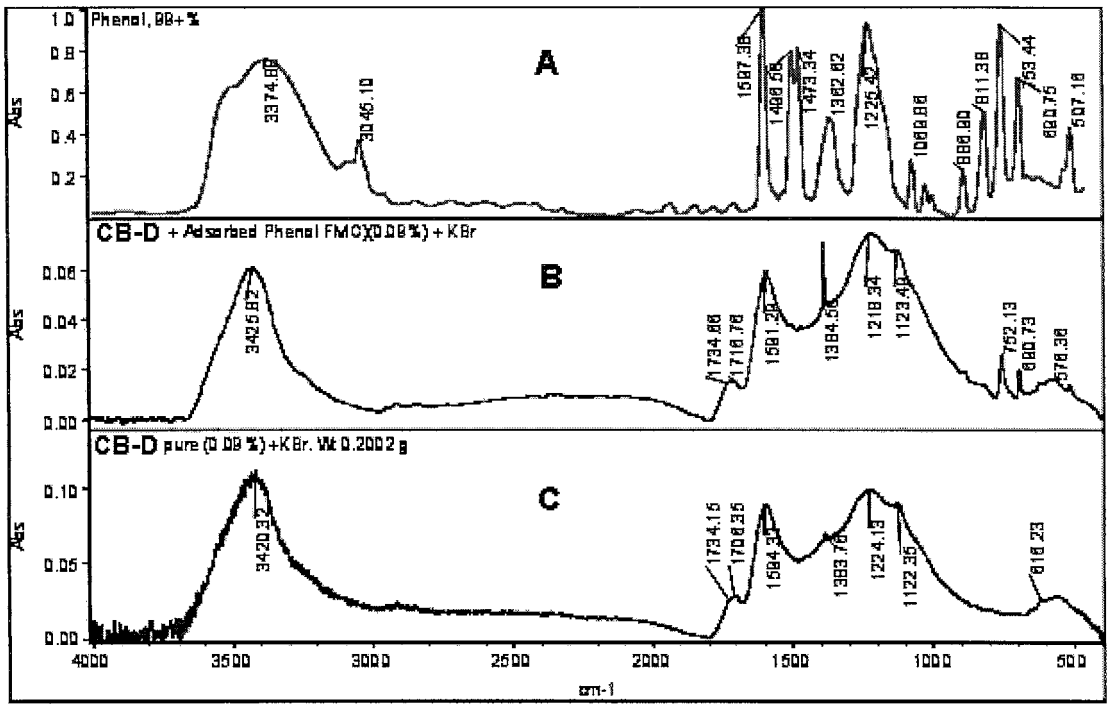

Figure 12 FTIR spectra of (a) pure phenol, (b) CB-D treated in the FMC with phenol and (c) CB-D carbon black.

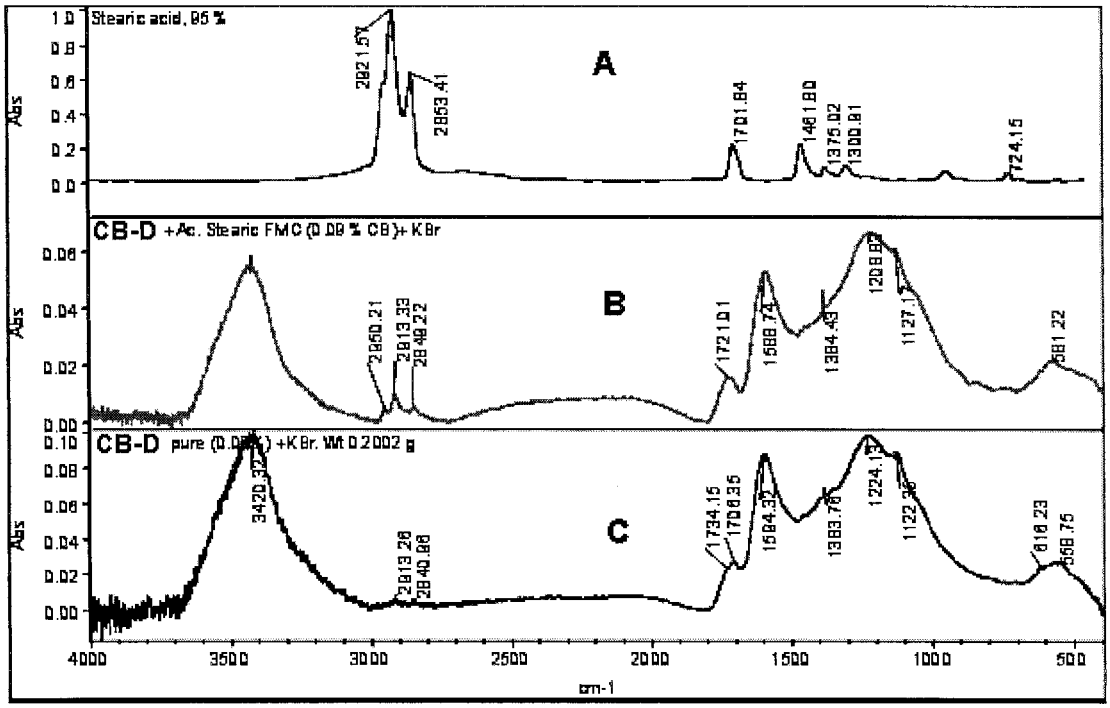

Figure 13 FTIR spectra of (a) pure stearic acid, (b) CB-D treated in the FMC with stearic acid and (c) CB-D.

carbon black. This shift is due to hydrogen bonding interactions between the carbonyl groups on the carbon black surface, and the amine hydrogen atoms. There is also a more significant shift to lower energy of the broad absorption centred at ca. 1584 cm^{-1}. This absorption is known to be related to the volatile content of the carbon blacks and may contain absorptions from carboxylates, α, β-unsaturated carbonyl species and phenols, that can also interact with the amine probes. Owing to the polyaromatic nature of the carbon black surface, significant levels of α, β-unsaturated carbonyl species may be expected.

3.3.2. FTIR spectra of carbon black treated in the FMC with carboxylic acids alcohols and ethyl acetate

In contrast to spectral data for the amine treated samples, the presence of adsorbed phenol was more easily detected on CB-D and CB-C. Absorptions at 752 cm^{-1} and 690 cm^{-1} can be obviously assigned to phenol adsorbed on CB-D (Fig. 12) whilst with CB-C some weak absorptions appear around 740 cm^{-1} and 700 cm^{-1}. Even CB-A and CB-B showed some evidence of adsorbed phenol, thus reflecting the strength of interaction with this probe.

Only CB-D (0.9%) shows presence of weakly adsorbed stearic acid with peaks at 2930 cm^{-1} (C–H stretching vibration of CH_2) (Fig. 13). The other probes could also be resolved on the carbon black surfaces, however, the absorptions were very weak, hence the spectra are not presented in the paper.

4. Conclusions

FMC and XPS were found to be complimentary techniques that can be used to investigate the interactions between carbon black and model compounds whose general structure is often found in stabilisers. Significant insight into factors affecting the adsorption of amines, alcohols, and carboxylic acids onto carbon black has been acquired.

In general, for amine model compounds, a greater basic character results in higher adsorption energy on a given carbon black, and stronger retention of the probe. The adsorption energy also depends on the structure of the amines. Greater values of adsorption energy are observed as dipole moment increases; in addition, simpler structures generally enable conformations which more interact energetically with the carbon black surface active sites, perhaps due to closer contact. Aromatic amines give higher than expected adsorption energies onto the purest sample of carbon black studied. This was thought to be due to flat adsorption, via dispersive interactions of the aromatic rings, with the planar graphene layers of this carbon black. The strong retention of the amine probes was thought to be due to acid base interactions and hydrogen bonding with surface phenolic species and carbonyl groups. The non-polar nature of the solvent together the strong basicity of the probes, may have resulted in interaction via an ion pair complex.

The difference in adsorption energy between carbon blacks towards the basic probes highlights differences in their surface chemistry. Due to the basic and nucleophilic character of the amine compounds, the higher activity of a given carbon black could be related to a greater presence of acidic adsorption sites per unit surface area on that carbon black. However, as with the previous two papers, a critical level of surface functional groups could be reached where strongly adsorbed atmospheric water together with mutual interactions between adjacent functional groups gave rise to a substantial reduction in adsorption activity.

Of the carboxylic acid, alcohol and ethylacetate series of probes, phenol was the most strongly adsorbing in terms of adsorption energy per unit area. In general the adsorption activity of this probe reflected the surface concentration of oxygen containing functional groups and the level of water present on the carbon blacks. As with the amine probe set, the hydrogel effect and mutual interaction between functional groups did cause a reduction in adsorption activity with the most highly functionalised carbon black. However, with the purest carbon black the heat of adsorption per unit area and per molecule of phenol, was higher than expected on the basis of the oxygen and water content. Therefore more energetic flat adsorption, as with the aromatic amines, was thought to occur.

The adsorption of carboxylic acids generally reflected the pH of the carbon blacks, with the most acidic of the carbon blacks adsorbing these probes least energetically. With the purest, and hence probably the smoothest surfaced, carbon black, molecular shape become the dominant factor influencing adsorption, with probes that are crystalline solids at ambient temperature (i.e., benzoic acid an stearic acid) showing higher than expected adsorption energies. This effect may be associated with either heats of crystallisation of these probes on the carbon black surface or flat adsorption which results in a significant increase in dispersive interaction.

The adsorption of aliphatic alcohols depended on their alkyl chain length as well as the surface chemistry of the carbon black. With the more acidic carbon blacks, the retention of alcohols increased, reflecting the amphoteric nature of the probe interacting with the carboxylic acid sites on the carbon blacks. In the absence of such adsorption sites, the adsorption energy, and degree of probe retention, reduced sharply as the energy contribution from hydrogen bonding interaction with carbon black surface phenolic OH and carbonyl groups, is far lower. Octadecanol gave a very interesting set of responses, which provided further evidence in support of adsorption of propanol within the pores of the oxidised carbon blacks. The high heat of adsorption of octadecanol (relative to propanol) on the purest carbon black is thought to be due to horizontal adsorption, or formation of ordered groups of adsorbed molecules on the purer carbon blacks.

Others stabilisers such as secondary antioxidants and UVA adsorbents have also been studied with the same carbon blacks and the results will be presented in a separate paper in this series.

Acknowledgements

The authors thank to The Cabot Corporation for financial support and the provision of materials for this programme of work.

References

1. J. M. PEÑA, N. S. ALLEN, M. EDGE, C. M. LIAUW, F. SANTAMARÍA, O. NOISET and B. VALANGE, *J. Mater. Sci.* **36** (2001) 2885.
2. J. M. PEÑA, N. S. ALLEN, M. EDGE, C. M. LIAUW, O. NOISET and B. VALANGE, *ibid.* **36** (2001) 4419.
3. A. I. MEDALIA, Medalia Associates, Inc., Carbon black, 1991.
4. J. B. DONNET, and C. M. LANSINGER, *Kautschuk Gummi Kunst.* **45** (1992) 459.
5. A. P. D'SILVA, *Carbon* **36** (1998) 1317.
6. J. B. DONNET, R. C. BANSAL and M. WANG, "Carbon Black, Science and Technology" (Marcel Dekker, Inc., New York, 1993).
7. M. H. POLLEY, W. D. SCHAEFFER and W. R. SMITH, *J. Am. Chem. Soc.* **73** (1951) 2161.
8. M. J. WANG, S. WOLFF and J. B. DONNET, *Rubber Chem. Technol.* **64** (1991) 714.
9. A. CONTESCU, C. CONTESCU, K. PUTYERA and J. A. SCHWARZ, *Carbon* **35** (1997) 83.
10. C. M. LIAUW, A. CHILDS, N. S. ALLEN, M. EDGE, K. R. FRANKLIN and D. G. COLLOPY, *Polym. Degrad. Stab.* **63** (1999) 391.
11. H. P. BOEHM, *Carbon* **32** (1994) 759.
12. R. H. BRADLEY, I. SUTHERLAND and E. SHENG, *Journal of Colloid and Interface Science* **179** (1996) 561.

13. K. PETER, C. VOLLHARDT and N. E. SCHORE, "Organic Chemistry," 2nd ed. (Freeman, NY, 1994).
14. B. WESSLÉN and M. KOBER, *Biomaterials* **15** (1994) 278.
15. E. ÖSTERBERG and K. BERGSTRÖM, *Applied Surface Science* **64** (1995) 197.
16. S. N. VINOGRADOV and R. H. LINNELL, "Hydrogen Bonding" (Van Nostrand Reinhold Company, New York, 1971).
17. T. ASAKAWA, K. OGINO and K. YAMABE, *Bull. Chem. Soc. Jpn.* **58** (1985) 2009.
18. T. J. FABISH and D. E. SCHLEIFER, *Carbon* **22** (1984) 19.
19. J. A. DEAN (ed.), "Handbook of Organic Chemistry" (McGraw Hill, NY, 1987) p. D–117.
20. *Idem.*, "Handbook of Organic Chemistry" (McGraw Hill, NY, 1987) E-51.

Received 24 July 2000
and accepted 16 January 2001